77-84

CONF-770649--1

LOW-TEMPERATURE IRRADIATION OF NIOBIUM WITH 15-MeV NEUTRONS*

H. R. Kerchner, R. R. Coltman, Jr., C. E. Klabunde, and S. T. Sekula
Solid State Division, Oak Ridge National Laboratory
Oak Ridge, Tennessee 37830

ABSTRACT

Niobium was irradiated at 4.2 K with high-energy d-Be neutrons to a fluence of 3.7×10^{15} n/cm^2. The neutrons were generated at the Oak Ridge Isochronous Cyclotron by the breakup reaction of 40-MeV deuterons in a thick Be target. The resulting neutron energy spectrum was broadly peaked near 15 MeV. The .012-cm-diameter wire sample (RRR = 200) was situated in a uniform transverse magnetic field. The critical current, flux-flow resistance, and normal-state resistance were measured by using a standard four-terminal technique. The critical-current density and flux-flow resistivity were observed to increase with irradiation and to decrease toward the preirradiation values with subsequent isochronal annealing between 4.2 K and 360 K. Using recent theories of flux-line-lattice deformation, we deduce the elementary pinning force and compare the result to theoretical calculations.

---

*Research sponsored by the Energy Research and Development Administration under contract with Union Carbide Corporation.

LOW-TEMPERATURE IRRADIATION OF NIOBIUM WITH 15-MeV NEUTRONS

H. R. Kerchner, R. R. Coltman, Jr., C. E. Klabunde, and S. T. Sekula

I. INTRODUCTION

We have investigated the influence of high-energy-neutron damage on flux-line motion in superconducting niobium in the mixed state. This investigation was part of an experimental study of the production and isochronal recovery of high-energy-neutron damage in three metals, copper, platinum, and niobium. The neutron-energy spectrum, experimental details, and the results of damage-resistivity measurements for all three metals are discussed elsewhere.[1,2] In this paper we present the results of measurements of the critical-current density and flux-flow resistivity for the niobium sample. Our results indicate that the high-energy-neutron damage contributes to flux-line pinning. Possible mechanisms for the interaction between the flux-line lattice and the high-energy-neutron damage are discussed, and theoretical results for the field dependence of the flux-line-pinning force are compared with the data. Finally, the observed isochronal recovery of the flux-line-pinning force is compared with the recovery expected on the basis of our theoretical model.

Each collision between a high-energy neutron and a niobium nucleus produces a cascade of Frenkel pairs. The strong similarity between the isochronal recovery of fission-neutron damage and that of d-Be-neutron damage in niobium[2] indicates that the density of Frenkel pairs approaches the saturation density within the cascades for both neutron spectra. The atomic fraction of primary knock-ons can be deduced from the dose Φ by using the spectrum-averaged cross section σ of 1.5 barns.[3] By using our measurement of the damage resistivity ρ_D and the measured value of the

saturation resistivity ρ_s,[4] one can estimate the average size of a cascade. Our estimates of the important dimensions characterizing the damage cascades in the niobium sample are summarized in Table I. These dimensions compare with the dimensions of the flux-line lattice in the following way: 1×10^{-6} cm $\lesssim$ cascade size $\lesssim$ isolated flux-line size $\lesssim$ flux-line-lattice parameter $\lesssim$ cascade spacing $\sim 2 \times 10^{-5}$ cm. The order of the relative dimensions makes this system a candidate for analysis by assuming a random distribution of point pins. However, caution is in order because all the dimensions are within about a factor of twenty of each other. It is important to note that Kramer's test[5] for the applicability of a line-pinning model to a system of point defects is satisfied by this system.

II. FUNDAMENTAL PINNING INTERACTION

There are three mechanisms that one might expect to contribute to the fundamental interaction between flux lines and the defect cascades: the $\Delta\kappa$ interaction,[6] the first-order,[7] and second-order[8] elastic-energy interactions. We shall calculate here the magnitude of the $\Delta\kappa$ interaction using the Ginzburg-Landau equation for the free energy near the upper critical field H_{c2}. Using the results of Kramer and Bauer[7] and of Toth and Pratt[8] for spherical inclusions, we find that the elastic-energy interactions are about a factor of 100 smaller than the $\Delta\kappa$ interaction.

If the Ginzburg-Landau order parameter Ψ is perturbed only slightly from its equilibrium value by the presence of the cascade, the energy of interaction between the cascade and the flux-line lattice can be calculated by first-order perturbation theory. To first order, the interaction energy is given by[6]

$$\Delta E = \frac{1}{4\pi} \int H_c^2 [-(H'_{c2}/H_{c2} - 1) |\psi|^2 + \tfrac{1}{2} (\kappa'^2/\kappa^2 - 1) |\psi|^4] dV \qquad (1)$$

where H_c (=1580 Oe at 4.2 K) is the thermodynamic critical field, κ is the Ginzburg-Landau parameter, and ψ is the relative order parameter. The primes refer to values in the damaged region, and the integral is taken over the volume of a cascade. The upper critical field H_{c2} is known to increase by 1.53 Oe/nΩ-cm with neutron damage.[9] Assuming that the resistivity within the cascade approaches the saturation value of 5 $\mu\Omega$-cm,[4] we find $H'_{c2}/H_{c2} = \kappa'/\kappa = 3.7$.

Since the size of the cascade is smaller than the flux-line-lattice parameter, $|\psi|^2$ can be taken out of the integral. Near H_{c2}, $|\psi|^2 = (1-B/H_{c2})F(\vec{x})$, and the spatially varying function $F(\vec{x})$ can be approximated by its first harmonic.[10] Then

$$\Delta E = \frac{1}{4\pi} H_c^2 V(\kappa'/\kappa - 1)(1-B/H_{c2})[-F(\vec{x}) + \tfrac{1}{2}(\kappa'/\kappa + 1)(1-B/H_{c2})F^2(\vec{x})] \qquad (2)$$

where V is the cascade volume. The spatial dependence of ΔE is illustrated in Fig. 1*a*. Each flux line sits in the center of a hexagonal unit cell (light lines). If the cascade were placed at the center of the flux line, ΔE would have a local maximum (ΔE=0). The straight lines between the lattice planes are roughly equipotentials. They intersect at saddle points at the center of each side of the unit cell. Near H_{c2} (i.e., $\frac{1}{2}[\kappa'/\kappa+1][1-B/H_{c2}] \ll 1$) the corner of a unit cell is a minimum ($\Delta E = -\frac{3}{8\pi} H_c^2 V [\kappa'/\kappa - 1][1-B/H_{c2}]$). As the flux density is lowered, the potential ΔE in the region of the unit-cell boundary becomes flat. At lower flux densities, the corners of the unit cell become maxima, and a circular valley develops inside the unit cell around the flux line.

The elementary pinning force is the derivative of ΔE with respect to a displacement of the flux-line lattice past a pinning defect (or

equivalently a displacement of the defect through the flux-line lattice). In Fig. 1*b* the maximum elementary pinning forces are plotted for our average cascade moving through the flux-line lattice in three ways as shown in Fig. 1*a*: directly toward the flux-line center, and from minimum to minimum through the saddle point at low fields and at high fields. For flux densities $b > .8H_{c2}$, the repulsive force near the flux-line core appears to dominate, while at lower flux densities the attractive force near the boundary of the unit cell dominates. It should be noted that a soft flux-line lattice can deform to reduce the effect of the repulsive force, but the maximum force between a cascade and the flux-line lattice must be at least as large as that associated with motion through the saddle point.

The volume pinning force F_p must be related to the elementary pinning forces f_p by a statistical theory that takes into account flux-line-lattice relaxation. Labusch has rigorously related F_p to f_p for a dilute system of point pins.[11] He obtains

$$F_p = Ndf_p^2 \frac{(B/\phi_o)^{\frac{3}{2}}}{8\sqrt{\pi}} \frac{1}{\sqrt{C_{44}}} \left[\frac{1}{\sqrt{C_{11}}} + \frac{1}{\sqrt{C_{66}}}\right] \qquad (3)$$

where C_{11}, C_{44}, and C_{66} are the elastic moduli of the flux-line lattice in Voigt's notation, ϕ_o is the flux quantum, N is the density of defects (i.e., cascades), and d is the size of a defect (cascade).

Schmucker and Brandt[12] recently proposed a modification to Labusch's theory that results in a larger value for F_p near H_{c2}. Their result is more complicated than Labusch's, and the simplifying approximations they make are not appropriate to niobium. Therefore, we will not make a detailed comparison between our data and their theory at this time.

The understanding of the effects of flux-line-lattice relaxation is not on such firm grounds when the pinning defects are not points or are not

dilute. Kramer has developed a theory of pinning by line defects parallel to the flux lines and has pointed out that a sufficiently dense system of point pins behaves the same as a system of line pins.[5] For a sufficiently dense system of point pins, he obtains

$$F_p = KN^4 f_p^4 B^{1/2}/C_{66}^3 \tag{4}$$

where K is approximately a constant. The line-pinning model should apply when the number of pinning defects intercepted by a unit length of a single flux line is greater than a critical density,

$$L^{-1} \geq L_c^{-1} = (C_{66} B/C_{44} \phi_0)^{1/2} . \tag{5}$$

In our sample, $L^{-1} = N\pi r^2 = 2.4 \times 10^4$ cm^{-1} where r is the flux-line radius, about 5×10^{-6} cm. In comparison, $L_c^{-1} \leq 1.0 \times 10^4$ cm^{-1} for our sample. Thus, Kramer's criterion for line pinning is satisfied by the cascades, even if pinning defects present in the sample before irradiation are neglected. To analyze our data, we shall use both Labusch's model and Kramer's model and compare the results.

III. EXPERIMENT

The high-energy neutrons were generated at the Oak Ridge Isochronous Cyclotron by the breakup reaction of 40-MeV deuterons in a thick Be target. The resulting neutron-energy distribution was broadly peaked near 15 MeV. The neutron source[13] and the neutron-energy distribution[1] at the sample have been described elsewhere.

The sample was a wire drawn from high-purity niobium to a diameter of 1.2×10^{-2} cm. The wire was mounted in an "M"-shaped groove in an anodized-aluminum plate (Fig. 1 of reference 2), which was stacked with plates holding the copper and platinum samples, one behind the other along the beam

axis, as shown in Fig. 2. The irradiation and the measurements were carried out with the samples immersed in liquid helium at 4.2 K. Also immersed in liquid helium and in line with the deuteron beam was a superconducting solenoid capable of producing a transverse field of 8 kOe at the sample. Detailed calculations showed that the field was uniform to within 4% over the volume occupied by the sample.

For annealing, the sample was raised into an annealing chamber in the Dewar (Fig. 3 of reference 2). The isochronal annealing program consisted of 5-minute pulses and increments of 5.2% of the absolute temperature from 8 K to 400 K. Measurements of the superconducting properties were made after the 50 K, 95 K, and 360 K pulses.

The relation between the current I and the potential V of the sample was measured by using conventional four-terminal techniques. The applied magnetic field was determined by measuring the magnet current and using a calculated conversion factor. The quantities of interest are indicated on a typical V(I) curve in Fig. 3. The flux-flow resistance R_f is the slope of the V(I) curve in the linear region. The lossless portion of the total current I, or the "pinning current," $I_p(V) = I - V/R_f$ is a function of voltage, but it approaches a constant value I_{po} at high voltages. The critical current I_c for the onset of flux motion was taken to be the current that produced a 1-μV potential drop across the sample.

Since we wanted to investigate as much of the V-I-H relation as possible in a limited period of time, we made three different types of measurements. Finely grained V(I) curves were determined at four magnetic fields in the mixed state. The critical current I_c was measured at about ten fields. Finely grained V(H) curves were determined at five currents. The last set of measurements are difficult to interpret because of the

nonlinear V(I) relation, but they could be made more quickly (hence more finely grained) than an $I_c(H)$ curve, and they produced our only evidence for the existence of a peak in I_c very near H_{c2}.

IV. RESULTS AND DISCUSSION

A. Flux-Flow Resistance

In this experiment, the defect cascades contribute about 6% to the normal-state resistance R_n after the irradiation. Near H_{c2} the superconducting electrons constitute only a small perturbation to the normal electrons. Therefore, the flux-flow resistance R_f is determined mainly by the normal-state resistance. In particular, R_f must change upon irradiation and annealing approximately in proportion to R_n. In contrast, at low fields dissipation takes place mainly in the flux-line core. If the interaction between a flux-line and a cascade is repulsive, the flux lines tend to avoid the cascades, so that the dissipation occurs mainly in the lower-resistivity material surrounding the cascade. Then R_f should not change by as much as R_n. On the other hand, if the interaction is attractive, R_f should change by more than R_n.

Our results indicate that for flux densities below roughly 0.7 H_{c2} the irradiation did not alter the flux-flow resistance. At higher flux densities, R_f was proportional to R_n. The effect is illustrated in Fig. 4. All measurements of R_f at each of the lower two flux densities were identical to within the experimental precision of 2%. All values of R_f/R_n at each of the higher two flux densities were identical to within 2%. In the figure, R_{fo} and R_{no} are the flux-flow and normal-state resistances before the irradiation; the lower part of the figure shows the dependence of the ratio of these quantities on the reduced flux density. In the upper part of the

figure, the changes in R_f with irradiation and annealing are compared with the changes in R_n. The straight lines indicate the increase in R_f with increasing R_n if R_f/R_n is assumed to remain constant. The data indicate that, for $B < 0.7\ H_{c2}$, the flux-line cores largely avoid the cascades.

B. Critical Current

Our results of the measurements of the critical current I_c before and after irradiation are shown in Fig. 5. There the volume pinning force $F_P = \frac{1}{c} J_c B$ is plotted, where J_c is the critical-current density deduced from the critical current I_c. For this sample, the flux density B was estimated by using the reversible magnetization curve for a dilute NbTa alloy that had been investigated previously.[14] The NbTa sample had a similar resistivity and an upper critical field H_{c2} within 1% of the value of H_{c2} for this Nb sample.

An important feature of these $I_c(B)$ and $F_p(B)$ relations is a narrow peak at $B \gtrsim 2600$ G. Clearer evidence for the existence of this peak is the dip in the V(H) curve (Fig. 6) that arises from a peak in $I_p(V)$. The peak in $I_p(V)$ presumably is associated with a peak in I_c. Although there is a dip in only one V(H) curve in Fig. 6, all such curves show an abrupt change of slope at the same field. A plot (not shown here) of the difference in V/V_n between any two of the curves of Fig. 6 also shows a peak at the same field. (Taking this difference cancels the current associated with flux flow and thereby clarifies the field variation of the pinning current.)

The value of H_{c2} that we used for our data analysis was determined from Fig. 6. The V(H) curves have a constant slope for fields just larger than the field where the dip occurs, but smaller than 2840 Oe. The value $H_{c2} = 2840$ Oe agrees well with the value for high-purity niobium[15]

corrected by 1.53 Oe/nΩ-cm[9] for the residual resistivity (before irradiation) of this sample.

An important test to be applied to the critical-current data is whether they satisfy a scaling law. That is, can I_c (or F_p) be expressed as a product of a function that depends only on field and another function that depends only on treatment? The result of the scaling-law test is illustrated in Fig. 7, where the field dependence of the ratio of the critical current I_c to the critical current I_{co} before irradiation is plotted. The ratio should show no field dependence if I_c obeyed a scaling law. Although such a scaling law cannot be applied at low flux densities or near H_{c2}, there is a broad region, 1200 G $\leq$ B $\leq$ 2200 G, where I_c/I_{co} is indeed nearly constant. The applicability of a scaling law suggests that flux-line pinning in this intermediate-field region is dominated by the repulsive interaction between flux lines and defect cascades (i.e., the $|\psi|^2$ term in the interaction energy), which has a field dependence similar to the field dependence associated with most other types of pinning defects.

It is suggested by Fig. 7 and borne out by calculations that the quantity $(I_c - I_{co})/I_{c1} - I_{co})$, where I_{c1} is the critical current after irradiation, is nearly field independent for the measurements of I_c after annealing. This last result suggests that the effect of pinning defects present in the sample before irradiation must have a different field dependence than the effect of the cascades for B < 1200 G and B > 2200 G.

Similar tests have been applied to our measurements of the flux-flow pinning current I_{po}. Although there are fewer data, and the uncertainty associated with I_{po} is larger, all of the above comments on a scaling law for I_c also are consistent with the measurements of I_{po}.

C. Elementary Pinning Forces

The field dependence of the elementary pinning force of an average cascade deduced from the critical-current measurements is shown in Fig. 8. Two sets of results are shown, one set obtained using Eq. 3 (Labusch's model) and one set obtained using Eq. 4 (Kramer's model). Values for the elastic moduli were calculated from the NbTa magnetization curve using Brandt's[16] formula for C_{66} and Labusch's relations[17] for $C_{11}-C_{66}$ and C_{44}. The value of f_p is determined by Kramer's model only to within the factor $K^{-\frac{1}{4}}$. For each model, the contribution to I_c of pinning defects present before irradiation was subtracted in the way appropriate to the model.

The results for both models show a sharp increase in f_p at low flux densities that presumably is associated with the attractive interaction calculated in Section II. Since this increase occurs at a lower flux density than it did in the calculation, we must conclude that our estimate for κ'/κ was slightly too high.

Kramer's model predicts a peak in I_c near H_{c2} even for an elementary pinning force f_p that decreases linearly with $(1-B/H_{c2})$. Thus, the flux-density dependence of f_p near H_{c2} deduced using Kramer's model is consistent with our calculation of the repulsive interaction, which is approximately proportional to $(1-B/H_{c2})$ and dominates near H_{c2}. Labusch's model requires a peak in f_p near H_{c2} to explain the peak in I_c. Figure 1 shows that such a peak arises from the force associated with defect motion from minimum (of ΔE) to minimum through the saddle point; however, this peak is too small to explain the observations. The model of Schmucker and Brandt predicts a sharp rise in I_c as the field is lowered from H_{c2} and may

adequately account for the data (although their estimates for high-κ materials predict no peak near H_{c2}).

The elementary pinning force recovers more than the sample resistance with low temperature annealing. Measurements for three annealing temperatures are plotted in Fig. 9. These results are for a single flux density in the range where a scaling law appears to work well and where the repulsive interaction appears to dominate. The pinning force due to the cascades f_p is normalized by its value f_{p1} before annealing. While Kramer's model was assumed in deriving these results, the values of f_p/f_{p1} are nearly model independent. The elementary pinning force associated with I_{po} behaves similarly to that associated with I_c, although it is much larger and recovers slightly less at low temperatures. In the intermediate-field region, where a scaling law applies, the critical current I_c recovers upon annealing at 360 K to a value slightly less than its value before irradiation (thus the negative f_p).

For comparison we have plotted the theoretical recovery of the repulsive and attractive pinning forces calculated under the assumption that $\kappa'/\kappa-1$ is proportional to the damage resistivity remaining. Both theoretical curves are normalized by the theoretical attractive interaction before annealing. Surprisingly, the recovery of the attractive interaction matches the data rather well in spite of the fact that the field dependence of f_p seems to require a dominant repulsive interaction at this flux density. If our estimate for κ'/κ was indeed too high and the repulsive interaction dominates at this flux density, then it follows that there must be some other reason for the rapid recovery of f_p at low temperatures.

V. SUMMARY AND CONCLUSIONS

We have measured the flux-flow resistance, critical current, and pinning current of a niobium sample irradiated at 4.2 K with 5-MeV neutrons. Changes in the flux-flow resistance can be understood on the basis of some simple qualitative ideas about the nature of the mixed state and a repulsive interaction between flux lines and defect cascades. The field dependence of the critical current and the pinning current can be understood with the help of Kramer's line-pinning model combined with our calculation of the interaction between defect cascades and flux lines based on Ginzburg-Landau theory. Use of Labusch's theory, although it gives the wrong field dependence near H_{c2}, provides agreement between theoretically calculated and experimentally measured critical currents to within a factor of two at intermediate flux densities. The isochronal recovery of the elementary pinning force f_p is more difficult to understand because it recovers more at low annealing temperatures than one expects on the basis of our model of the interaction combined with the experimental results for the field dependence of f_p.

We believe that the discrepancy between the field dependence of f_p and its isochronal recovery is due to complexities of the annealing process that we have not taken into account. For example, the resistivity change measured during recovery may not be a direct measure of the decrease in the localized resistivity within a cascade. Further investigation of the recovery of the flux-line-pinning force of defect cascades is in order. Since flux lines probe the cascades in a special way, additional studies may yield information that cannot be obtained by normal-state resistivity measurements.

Table I. Characteristics of High-Energy-Neutron Damage in This Experiment

Dose	$\Phi = 3.7 \times 10^{15}$ n/cm^2
Atomic fraction of primary knock-ons	$\sigma\Phi = 5.6 \times 10^{-9}$
Average distance between cascades	$(\sigma\Phi)^{-\frac{1}{3}} = 600$ lattice parameters $= 2 \times 10^{-5}$ cm
Saturation resistivity[4]	$\rho_s = 5$ μΩ-cm
Damage resistivity	$\rho_D = 3.74$ nΩ-cm
Volume of average cascade	$\rho_D/\rho_S\sigma\Phi = 1.3 \times 10^5$ atomic volumes $= 2.4 \times 10^{-18}$ cm^3
Size of average cascade	$(\rho_D/\rho_S\sigma\Phi)^{\frac{1}{3}} = 50$ lattice parameters $= 1 \times 10^{-6}$ cm

REFERENCES

1. J. B. Roberto, C. E. Klabunde, J. M. Williams, R. R. Coltman, Jr., M. J. Saltmarsh, and C. B. Fulmer, Appl. Phys. Lett. 30, 509 (1977).

2. J. B. Roberto, C. E. Klabunde, J. M. Williams, and R. R. Coltman, Jr., to be published in J. Nucl. Mater.

3. Calculated by J. B. Roberto using the neutron spectrum given in Ref. 1.

4. B. S. Brown, T. H. Blewitt, T. L. Scott, and A. C. Klank, J. Nucl. Mater. 52, 215 (1974).

5. E. J. Kramer, J. Appl. Phys. 44, 1360 (1973).

6. A. M. Campbell and J. E. Evetts, Adv. Phys. 21, 333 (1972).

7. E. J. Kramer and C. L. Bauer, Philos. Mag. 15, 1189 (1967).

8. L. E. Toth and I. P. Pratt, Appl. Phys. Lett. 4, 75 (1964).

9. B. S. Brown, Proceedings of the International Discussion Meeting on Flux Pinning in Superconductors, St. Andreasburg, Germany (September 1974), Akademie der Wissenschaften, Göttingen, 1975.

10. D. Saint-James, E. J. Thomas, and G. Sarma, Type II Superconductivity, p. 61, Pergamon Press, New York, 1969.

11. R. Labusch, Crystal Lattice Defects 1, 1 (1969).

12. R. Schmucker and E. H. Brandt, Phys. Status Solidi B 79, 479 (1977).

13. M. J. Saltmarsh, C. A. Ludemann, C. B. Fulmer, and R. C. Styles, Oak Ridge National Laboratory Report ORNL/TM-5696 (Oak Ridge, Tenn., 1976).

14. J. R. Clem, H. R. Kerchner, and S. T. Sekula, Phys. Rev. B 14, 1893 (1976).

15. D. K. Finnemore, T. F. Stromberg, and C. A. Swenson, Phys. Rev. 149, 231 (1966).

16. E. H. Brandt, Phys. Status Solidi B 77, 551 (1976).

17. R. Labusch, Phys. Status Solidi 32, 439 (1969).

FIGURE CAPTIONS

Fig. 1. (a) Flux-line lattice shown with unit cells (light lines) and equipotentials (heavy lines) for the interaction between the flux lines and a defect cascade. (b) The theoretical elementary pinning force of a defect cascade for a cascade moving with respect to the flux-line lattice in three directions as indicated by the arrows in (a).

Fig. 2. Detailed view of the irradiation chamber, shown with the samples in position.

Fig. 3. A typical current-voltage relation for the Nb sample before irradiation.

Fig. 4. (a) Comparison between the behavior of the flux-flow resistance and the behavior of the normal-state resistance in Nb with irradiation and isochronal annealing. (b) The field dependence of the flux-flow resistance before irradiation.

Fig. 5. The flux-density dependence of the volume pinning force of Nb before and after low-temperature irradiation with 15-MeV neutrons.

Fig. 6. The field dependence of the flux-flow voltage of Nb before and after low-temperature irradiation with 15-MeV neutrons and after isochronal annealing.

Fig. 7. Test for the applicability of a scaling law to the critical current I_c of Nb. If I_c were a simple product of a function only of field and another function only of treatment, I_c/I_{co} would be field independent.

Fig. 8. The experimental elementary pinning force of the defect cascades derived from the data by using two different models for the summation of the forces.

Fig. 9. Comparison between the recovery of the elementary pinning force f_p of the defect cascades with isochronal annealing and that of the normal-state resistance R_n. The pinning force f_p is normalized by its value f_{p1} before annealing.

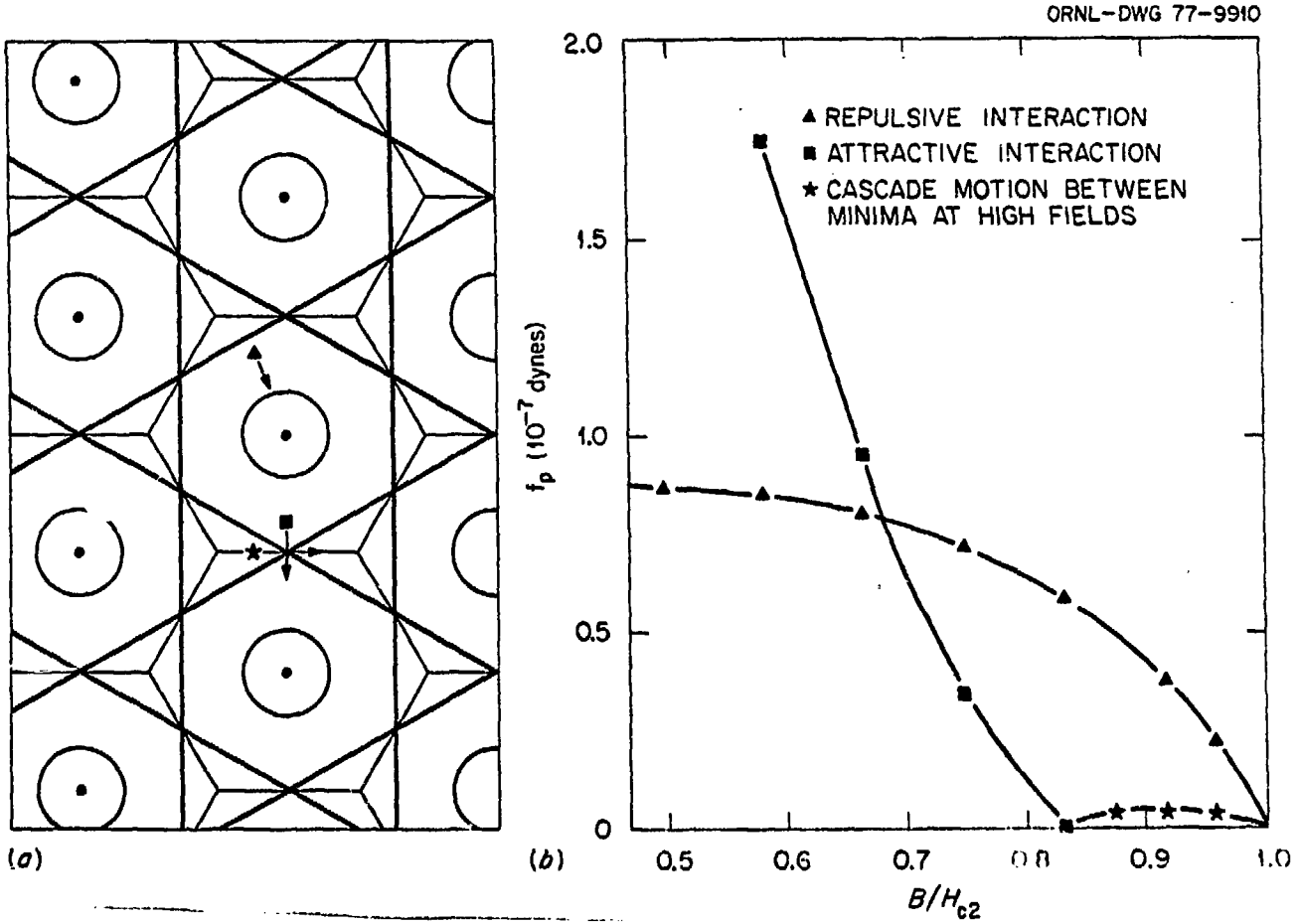

Fig. 1. (a) Flux-line lattice shown with unit cells (light lines) and equipotentials (heavy lines) for the interaction between the flux lines and a defect cascade. (b) The theoretical elementary pinning force of a defect cascade for a cascade moving with respect to the flux-line lattice in three directions as indicated by the arrows in (a).

ORNL-DWG 76-20239

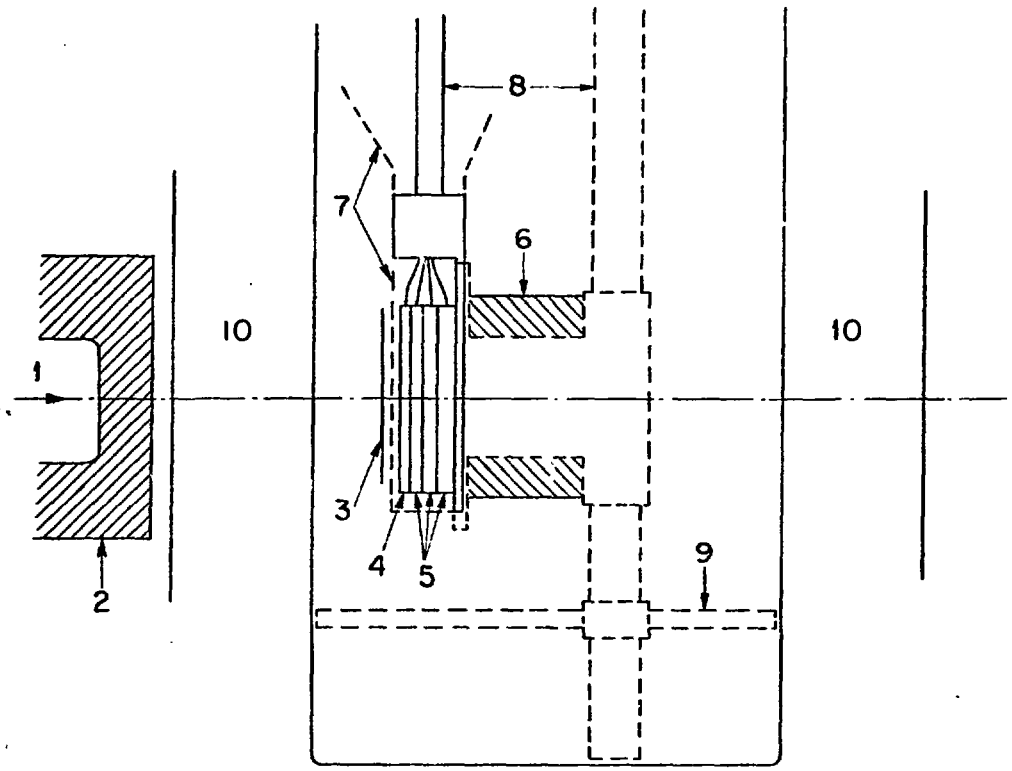

1 DEUTERON BEAM AXIS
2 Be TARGET (NEUTRON SOURCE)
3 DOSIMETER FOILS
4 DOSIMETER SAMPLE AND THERMOCOUPLE
5 INDIVIDUAL SAMPLE HOLDERS
6 MAGNET WINDINGS ON THIN ALUMINUM CORE
7 GUIDE FUNNEL FOR POSITIONING SAMPLES
8 THIN-WALL STAINLESS TUBING
9 EXPERIMENT POSITIONING SPIDER
10 DEWAR INSULATION (CONCENTRIC ALUMINUM HEAT SHIELDS IN EXPERIMENTAL REGION)

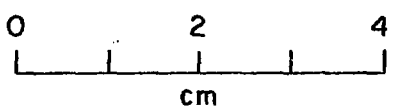

Fig. 2. Detailed view of the irradiation chamber, shown with the samples in position.

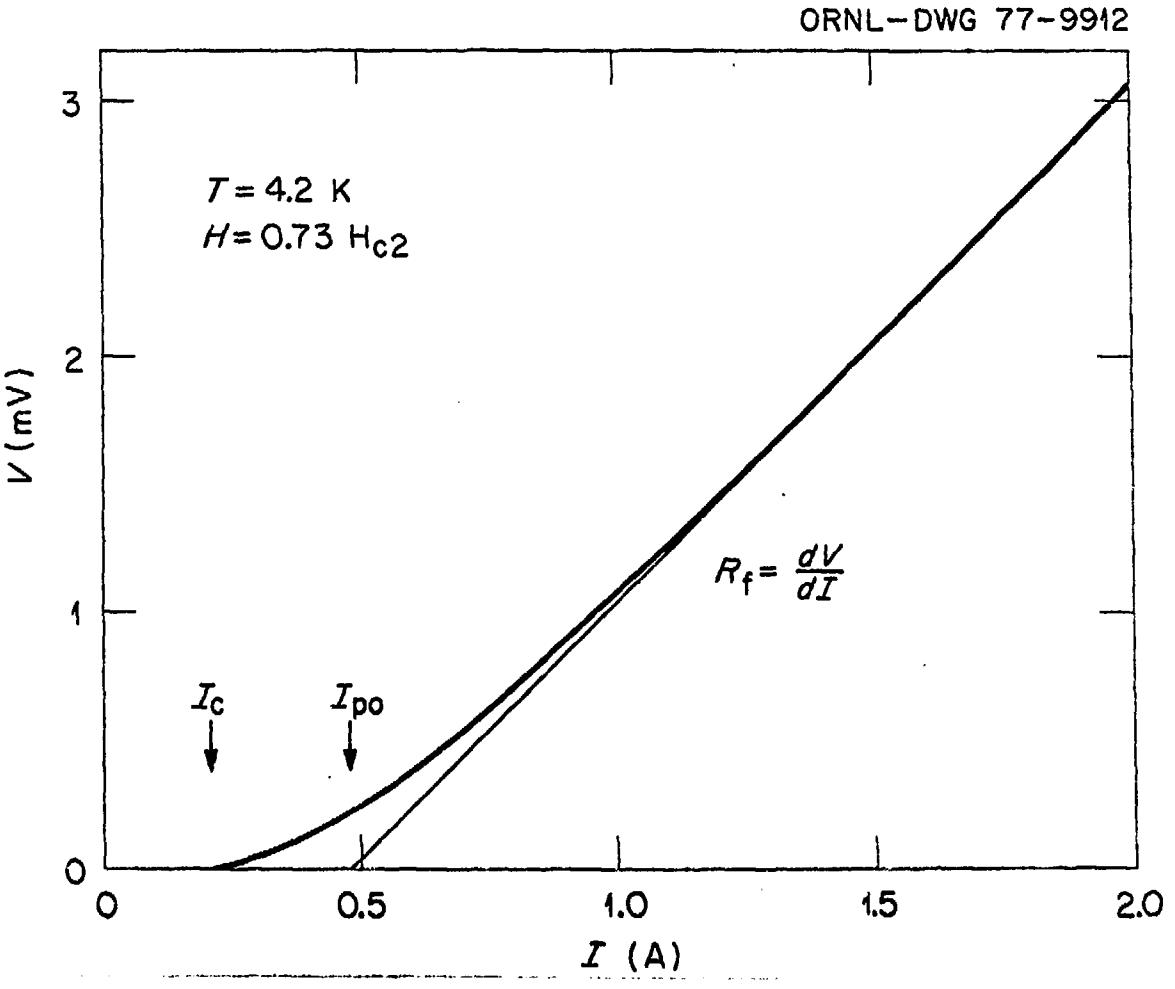

Fig. 3. A typical current-voltage relation for the Nb sample before irradiation.

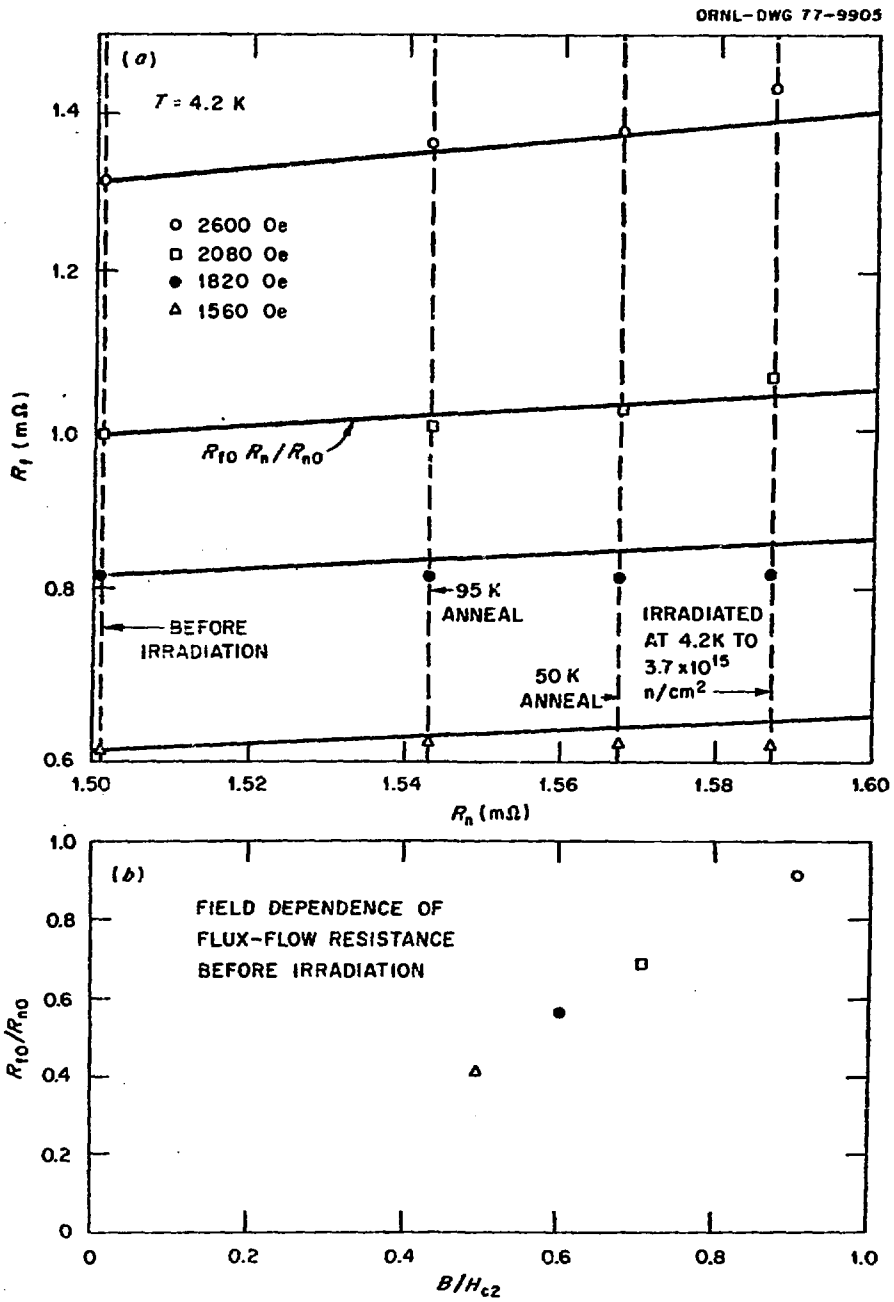

Fig. 4. (a) Comparison between the behavior of the flux-flow resistance and the behavior of the normal-state resistance in Nb with irradiation and isochronal annealing. (b) The field dependence of the flux-flow resistance before irradiation.

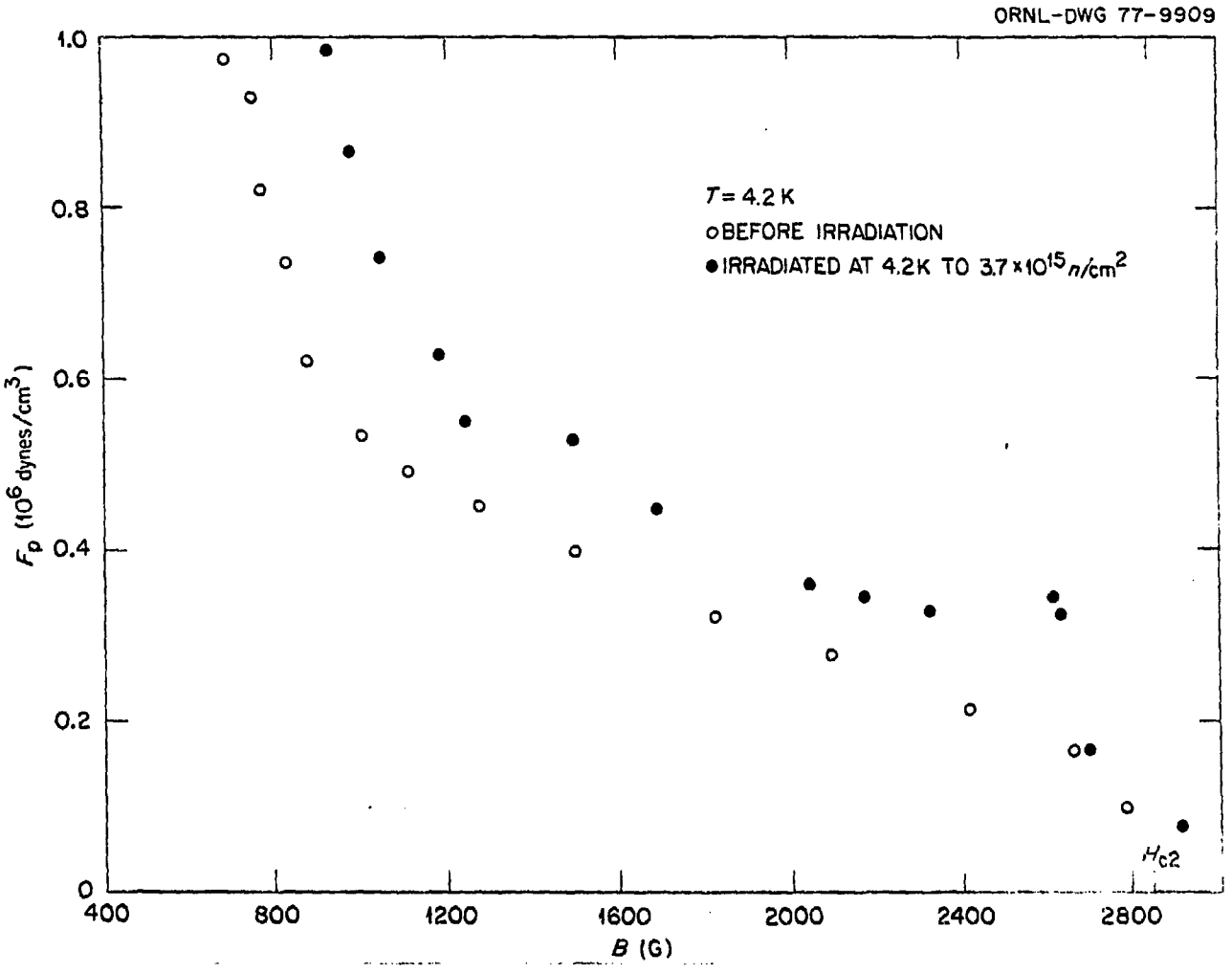

Fig. 5. The flux-density dependence of the volume pinning force of Nb before and after low-temperature irradiation with 15-MeV neutrons.

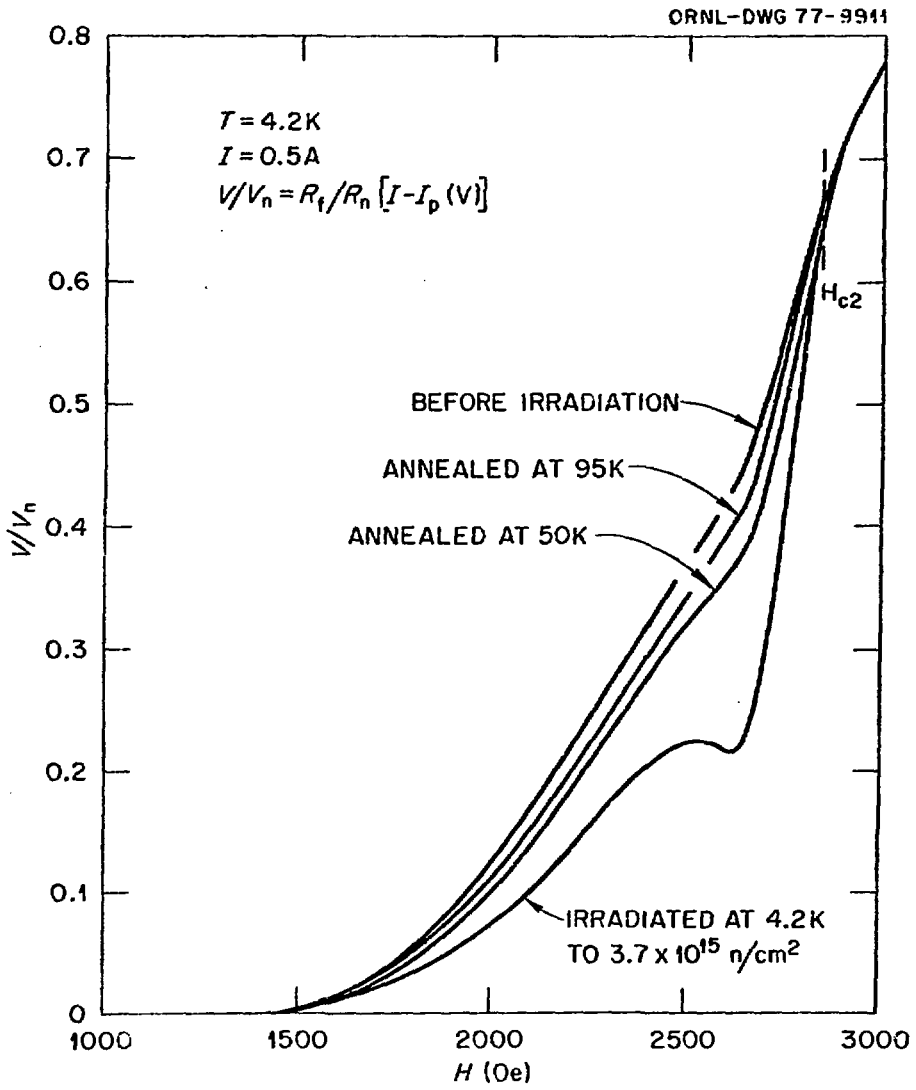

Fig. 6. The field dependence of the flux-flow voltage of Nb before and after low-temperature irradiation with 15-MeV neutrons and after isochronal annealing.

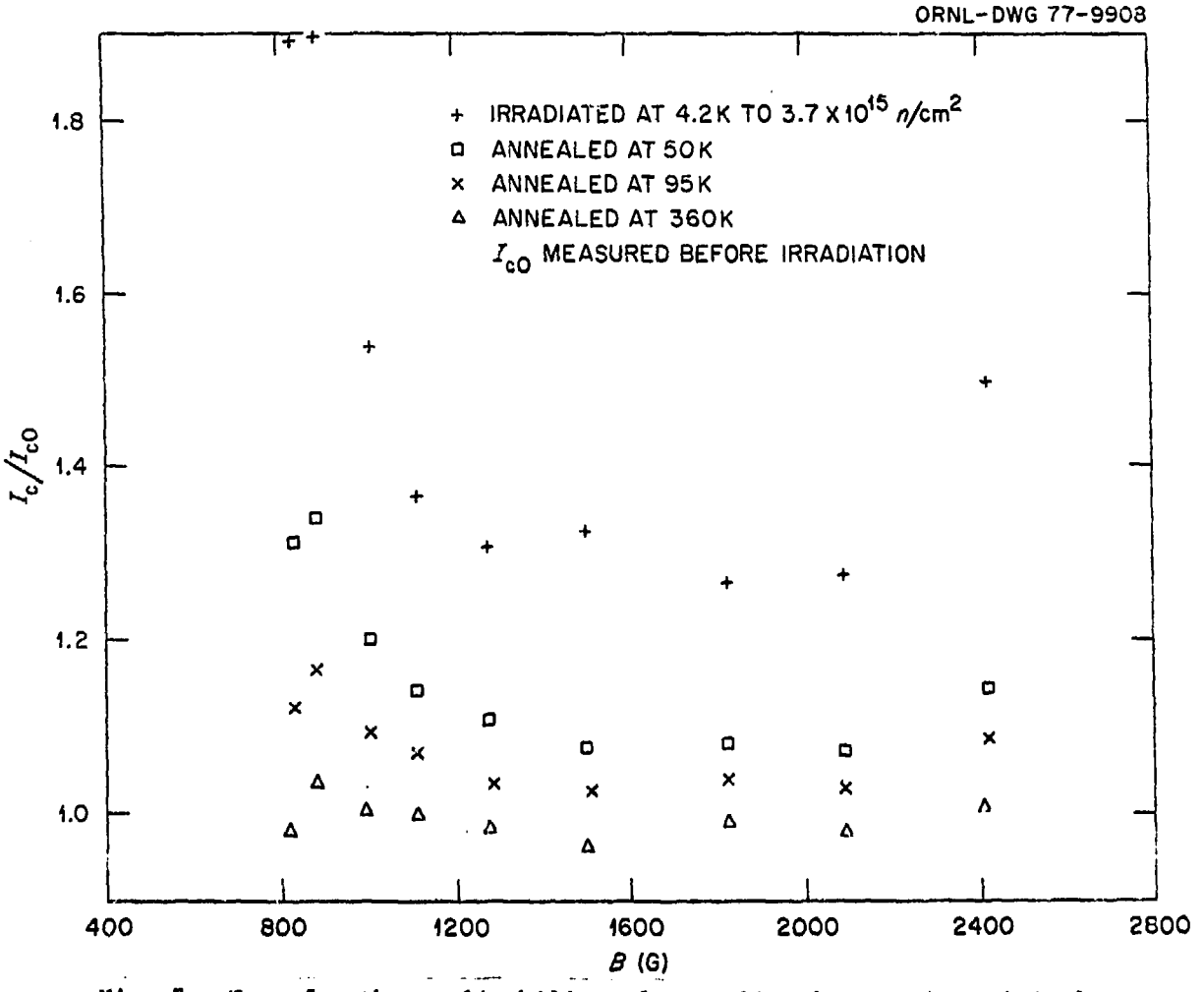

Fig. 7. Test for the applicability of a scaling law to the critical current I_c of Nb. If I_c were a simple product of a function only of field and another function only of treatment, I_c/I_{co} would be field independent.

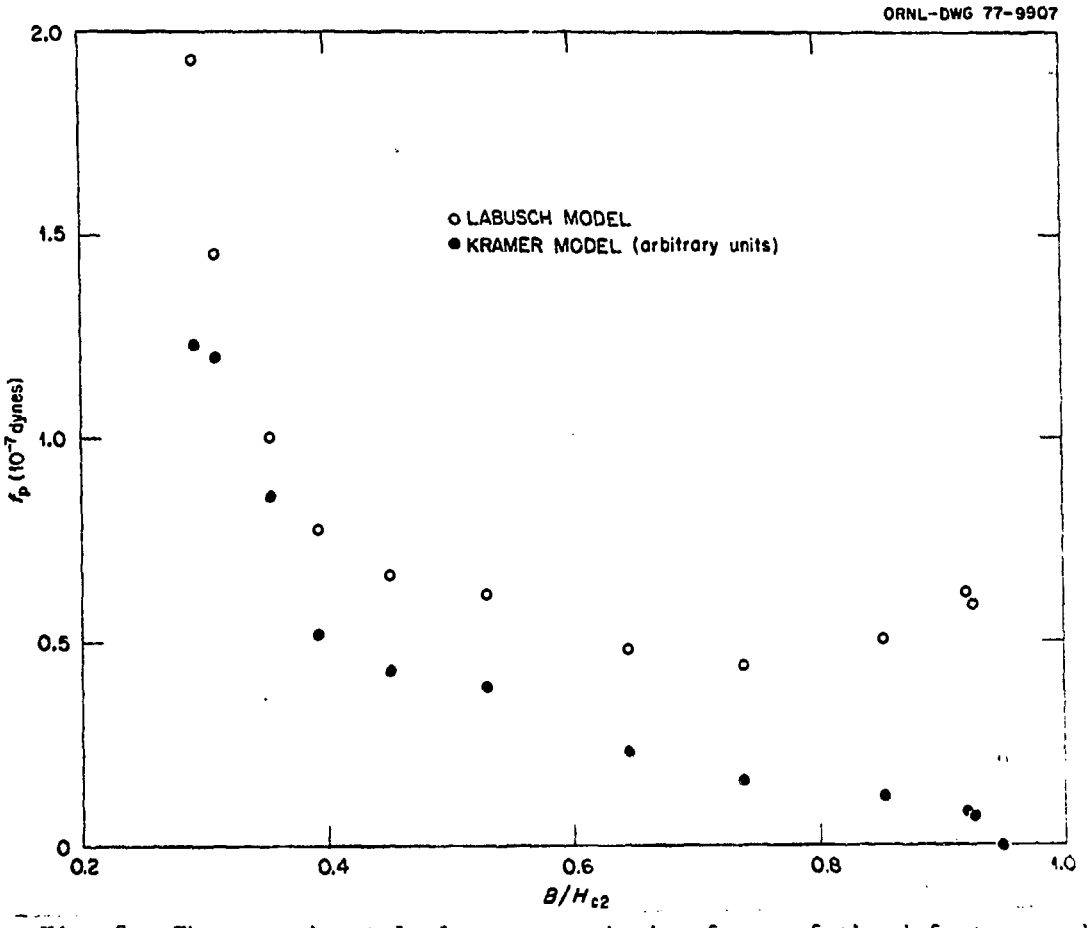

Fig. 8. The experimental elementary pinning force of the defect cascades derived from the data by using two different models for the summation of the forces.

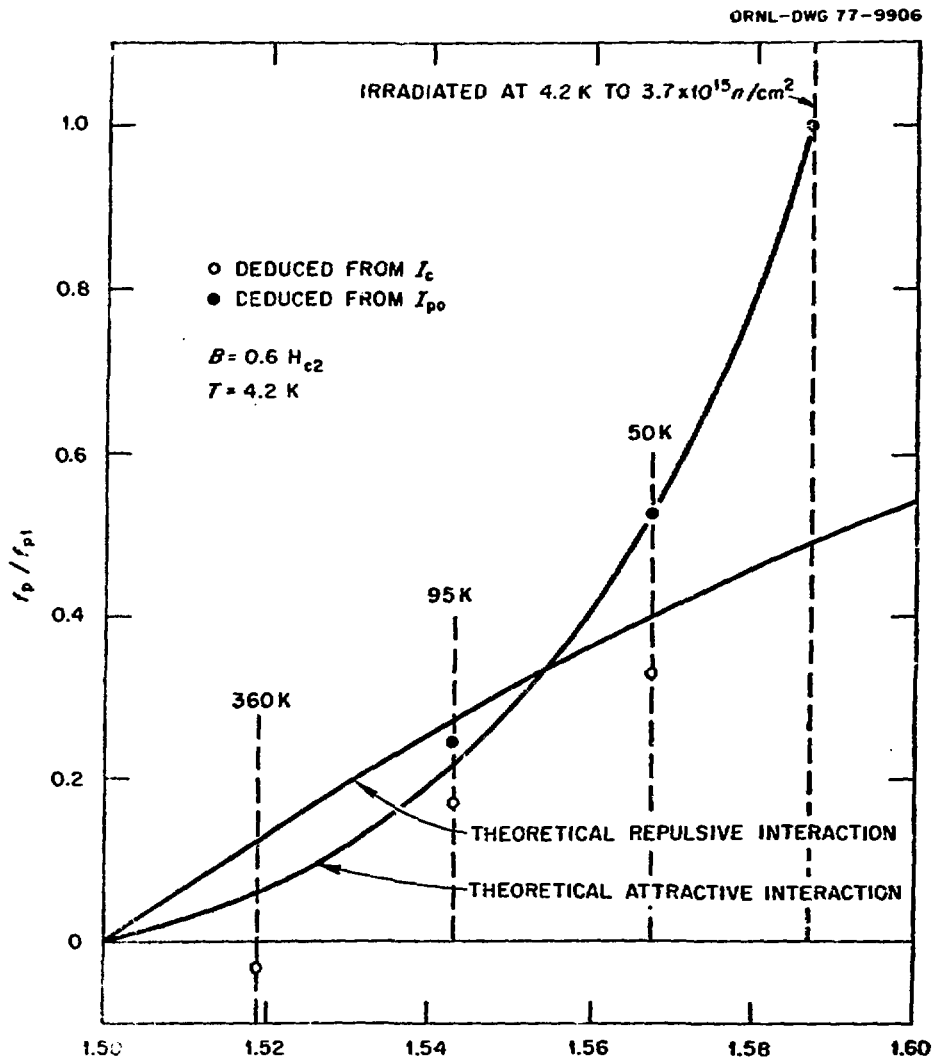

Fig. 9. Comparison between the recovery of the elementary pinning force f_p of the defect cascades with isochronal annealing and that of the normal-state resistance R_n. The pinning force f_p is normalized by its value f_{p1} before annealing.